

AUTHOR QUERY FORM

 ELSEVIER	Journal: EABE Article Number: 2656	Please e-mail or fax your responses and any corrections to: E-mail: corrections.esch@elsevier.macipd.com Fax: +44 1392 285878
------------------------------------------------------------------------------------------------------	---------------------------------------------------------	----------------------------------------------------------------------------------------------------------------------------------------------------------------------------------------------------------------------------

Dear Author,

Please check your proof carefully and mark all corrections at the appropriate place in the proof (e.g., by using on-screen annotation in the PDF file) or compile them in a separate list. Note: if you opt to annotate the file with software other than Adobe Reader then please also highlight the appropriate place in the PDF file. To ensure fast publication of your paper please return your corrections within 48 hours.

For correction or revision of any artwork, please consult <http://www.elsevier.com/artworkinstructions>.

Any queries or remarks that have arisen during the processing of your manuscript are listed below and highlighted by flags in the proof. Click on the [Q](#) link to go to the location in the proof.

Location in article	Query / Remark: click on the Q link to go Please insert your reply or correction at the corresponding line in the proof
Q1	Please confirm that given names and surnames have been identified correctly.
Q2	Please complete and update the reference given here (preferably with a DOI if the publication data are not known): Ref. [10]. For references to articles that are to be included in the same (special) issue, please add the words 'this issue' wherever this occurs in the list and, if appropriate, in the text.
Q3	Please check the address for the corresponding author that has been added here, and correct if necessary.
Q4	Please check the journal abbreviation in Ref. [10].
Q5	Please check the journal abbreviation in Ref. [36].
Q6	Figs. 7 and 10 have been submitted as color images; however, the captions have been reworded to ensure that they are meaningful when your article is reproduced both in color and in black and white. Please check and correct if necessary.

Thank you for your assistance.

Please check this box if you have no corrections to make to the PDF file



ELSEVIER

Contents lists available at [SciVerse ScienceDirect](http://www.sciencedirect.com)

Engineering Analysis with Boundary Elements

journal homepage: www.elsevier.com/locate/enganabound

On physical and numerical resonances for water wave problems using the dual boundary element method

Q1 I.L. Chen^a, J.W. Lee^b, Y.C. Hsiao^c, J.T. Chen^{b,d,*}

^a Department of Naval Architecture and Ocean Engineering, National Kaohsiung Marine University, Kaohsiung, Taiwan

^b Department of Harbor and River Engineering, National Taiwan Ocean University, Keelung, Taiwan

^c Institute of Applied Mechanics, National Taiwan University, Taipei, Taiwan

^d Department of Mechanical and Mechatronics Engineering, National Taiwan Ocean University, Keelung, Taiwan

ARTICLE INFO

Article history:

Received 16 December 2011

Accepted 16 April 2012

Keywords:

Scattering

Water wave

Dual boundary element method

Near-trapped mode

Fictitious frequency

ABSTRACT

Scattering problems of water waves impinging on bottom-mounted vertical cylinders are solved by using the dual boundary element method (DBEM). Both resonances due to near-trapped mode (physics) and fictitious frequency (mathematics) are examined. It is found that the near-trapped mode is a physical phenomenon and the fictitious frequency stems from the numerical instability. A trapped mode is associated with a singularity that lies on the real axis of complex wave number. A near-trapped mode means a localized behavior that energy is trapped in a truncated periodical structure. Critical wave number for the near-trapped mode and fictitious frequency of numerical instability are detected in this work. Numerical oscillation of the resultant force near the fictitious frequency is also observed by using the DBEM. Fictitious frequencies depend on the formulation instead of the specified boundary condition. Both the Burton and Miller approach and the CHIEF method are employed to alleviate the problem of irregular frequencies. Highly rank-deficiency matrices for four identical cylinders are numerically examined and the rank is promoted by adding valid CHIEF constraints. Parameter study of spacing and radius of cylinders on the near-trapped mode and fictitious frequency is also addressed. Several examples of water wave interaction by circular and square cylinders are demonstrated to see the validity of the present formulation.

© 2012 Elsevier Ltd. All rights reserved.

1. Introduction

For designing the offshore platforms mounted on the seabed, such as oil platforms which consist of a number of legs, it is important to understand the interaction between the vertical cylinders and water waves. For a scattering problem of plane waves impinging on vertical cylinders, a closed-form solution of force on a single vertical cylinder was derived by MacCamy and Fuchs [1]. A similar analysis extended to two cylinders was investigated by Spring and Monkmeyer [2]. They used the addition theorem to analytically derive the solution of wave scattering problems. Two cylinders of equal and unequal sizes subject to the incident wave of arbitrary angle were analyzed. They claimed that their method was a direct approach, since they formulated the problem by using a linear algebraic system and the solution was obtained easily from a single matrix inversion. A different method presented by Twersky [3] is called the multiple-scattering approach. In his approach, he

took one cylinder at a time and scattering coefficients were solved sequentially. Besides, the boundary conditions of the problem which they solved are also different. Duclos and Clément [4] proposed a simplified model under linearized theory to simulate the interaction between cylinders subject to an incident wave. Simon [5] as well as McIver and Evans [6] proposed an approximate solution based on the assumption that the cylinders are widely spaced. Later, Linton and Evans [7] also used the same approximate method as proposed earlier by Spring and Monkmeyer [2]. The main contribution was to provide a simple formula for the potential on the surfaces of the cylinders which makes the computation of forces much more straightforward. However, their results of four cylinders [7] were incorrect and corrigendum was given in Ref. [8]. Chen et al. [9] successfully employed the null-field integral equation approach to solve scattering problems of water wave across an array of circular cylinders. Based on the null-field integral equations in conjunction with degenerate kernels and Fourier series, the principal-value sense for singular integrals in boundary element method can be avoided. Only circular cylinders have been considered in Ref. [9], although elliptical case has been studied by Chen and Lee [10]. Extension to solve problems of general shape is not trivial by using the dual boundary element method (BEM).

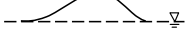
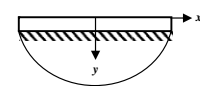
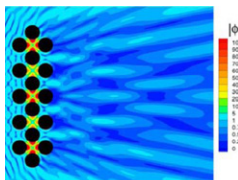
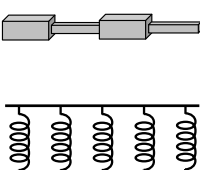
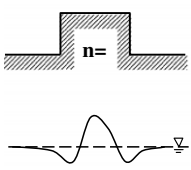
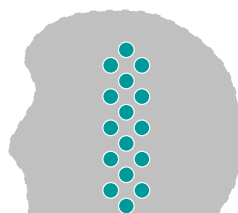
* Corresponding author at: Department of Harbor and River Engineering, National Taiwan Ocean University, Keelung, Taiwan.
E-mail address: jtchen@mail.ntou.edu.tw (J.T. Chen).

It is well known that periodical pattern may result in band gaps, trapped mode and local resonance. There are several sources for the periodical pattern, e.g., material distribution, geometric shape and boundary condition as given by Ref. [11] and Table 1 for a flexural beam. Trapped modes and near-trapped modes appear in different fields, such as flexural wave in beam vibration, hydraulics in civil engineering, Love wave in earthquake engineering, water wave in ocean engineering and bound state in quantum mechanics are summarized in Table 1. Here, we focus on the water wave. Near-trapped mode means a localized behavior that energy is trapped in a truncated periodical structure. A trapped mode is associated with a singularity that lies on the real axis of complex wave number. Water wave diffraction and near-trapped mode by a multi-column mounted structure were studied by Evans and Porter [12]. Near-trapped modes were found for the cases of four, five and six cylinders. The wave number to excite the near-trapped mode was numerically determined by detecting the real value of ka which results in the maximum force, where k and a are the wave number and the radius of cylinder, respectively. Sphaier and Yeung [13] solved the 3-D truncated cylinder problem of an infinite array before the two-dimensional (2-D) work of Linton and Evans [7] (bottom-mounted cylinders are 2-D problems), whereas Kashiwagi [14] reported a useful formulation for handling a very large number of cylinders with some periodical structures. Besides, experiments were conducted by Kashiwagi [15] and Kagamoto et al. [16]. The results were all in good agreement with the computed results using a linearized model. Also, theoretical, computational and experimental methods were investigated by Ohl et al. [17]. Time-dependent water-wave scattering by arrays of cylinders and the approximation of near-trapped mode were studied in a complex “ k ” plane by Meylan and Eatock Taylor [18]. Dirichlet and Neumann trapped modes of large number of cylinders (100) in an infinite domain were found to approach those of infinite number of cylinders by Maniar and Newman [19]. McIver and Evans [6] used an approximate method to estimate the wave forces for a group of five cylinders. Trapped modes for a semi-infinite domain were studied by Thompson et al. [20]. For multiple cylinders in a channel, trapped modes were also found by Evans and Porter [21]. Yao et al. [22] also examined the behavior at cut-off frequencies in a channel.

Mathematically speaking, the array-guided cylinders may result in non-trivial solutions of the homogeneous problem at particular values of wave number. It can be understood as eigen vectors corresponding to eigen values of certain differential operators on unbounded domains even though there is no characteristic length as mentioned by Linton and McIver [23]. A characteristic length is only available for a finite-domain problem.

We will study the near-trapped mode by using the DBEM. The DBEM has been successfully employed to solve scattering problems of plane wave [24], the vibration of membrane with a degenerate boundary [25], the vibration of membrane with multiply-connected domain problems [26] and the plate vibration [27]. By using the DBEM to solve the water wave problem, two kinds of peaks for the resultant force on the cylinder versus the wave number will be examined. One is the near-trapped mode in physics; the other is the irregular frequency in mathematics. Existence of the irregular frequencies stems from integral formulation for exterior Helmholtz problems. A near-trapped mode is physical phenomenon and a fictitious frequency stems from the numerical instability. Since near-trapped modes and fictitious frequencies both contribute peaks in the resultant force, how to recognize the source becomes an interesting and important issue. Dokumaci [28] and Juhl [29] both pointed out that numerical oscillation become serious as the number of boundary elements increases. The physical phenomenon in real practice depends on the boundary condition. But, the fictitious frequency is not physically realizable, it is imbedded in the adopted formulation of BIEM (singular integral equation or hypersingular integral equation). Fictitious frequencies depend only on the formulation instead of the specified boundary condition. A proof in continuous and discrete systems can be found in Ref. [30]. Regarding the fictitious frequency, two ideas of the Burton and Miller method [31] and the combined Helmholtz interior integral equation formulation (CHIEF method) [32], have been proposed to deal with this problem. The former one needs hypersingular formulation while the latter one may take risk once the CHIEF point falls on the nodal line of corresponding interior eigen modes. Based on the circulant properties and degenerate kernels, an analytical and numerical experiment in a discrete system of a cylinder was achieved [33]. The optimum numbers and proper positions for the

Table 1
Near-trapped modes in physics and engineering.

Engineering and physics in the trapped mode				
Vibration	Hydraulic engineering	Earthquake engineering	Coastal engineering	Quantum physics
				 <p>Bound state in quantum mechanics</p>
		<p>Love wave in a layer-elastic half-space</p>		
Beam vibration [11]	Trapped modes on a ridge		Near-trapped mode in water wave	

collocation of CHIEF points in the complementary domain are analytically studied [33]. The literature of using the CHIEF method to solve multiple radiators or scattering problems is very limited until now. Only two papers by Schenck [34] and Dokumaci and Sarigul [35] can be found to our knowledge. For Dokumaci and Sarigul's paper, it is questionable that extra CHIEF points excite another unsymmetric fictitious frequency although it can suppress the appearance of one symmetric fictitious frequency. For the oscillation of new fictitious frequency, the rank is not previously deficient if the CHIEF point is not added. Mathematically speaking, this is unreasonable since more constraint can improve the rank. Regarding the Schneck paper [34] for sonar applications using the Helmholtz integral equation, the details of how to choose the CHIEF point for two spheres was not clearly reported. For the single radiator or scatterer of 2-D case, the rank deficiency is at most 2 for a circular radiator or scatterer in case of a fictitious frequency. For the 3-D case of single radiator or scatterer, the rank deficiency may be higher, e.g., a sphere case. We may wonder what happens for the rank deficiency of multiple identical radiators or scatterers. This issue is also our interest since an array of cylinders in water wave is one kind of multiple scatterers. A more rigorous study to examine the serious rank-deficiency matrices due to multiple equal scatterers is our concern. Besides, the numerical experiment of extra CHIEF points to promote the rank will be numerically performed.

In this paper, we focus on the dual boundary element method to solve the scattering problem of water waves instead of solving the problem by using the null-field BIEM, due to its limitation of circular [9] or elliptical cylinder [10]. Without loss of the generality, we employ the dual BEM to revisit the water wave problem containing four square cylinders. Both the near-trapped mode (resonance in physics) and the fictitious frequency (resonance in mathematics) are addressed in this paper. The Burton and Miller method and the CHIEF method will be employed to deal with problems of numerical instability. In Section 2, we introduce the formulation of dual boundary integral equation for the water wave problem. Regularization techniques for the fictitious frequencies, the CHIEF method and Burton and Miller approach, are both implemented in Section 3. Some examples including one-circular cylinder, four circular cylinders and four square cylinders are demonstrated to verify the validity of the Burton and Miller approach and the CHIEF method.

2. Problem statement and integral formulation

2.1. Problem statement

Now we consider an array of four circular cylinders mounted at $z = -h$ upward to the free surface as shown in Fig. 1. The governing equation of the total velocity potential $\Phi(x_1, x_2, z; t)$ satisfies the Laplace equation as shown below:

$$\nabla^2 \Phi(x_1, x_2, z; t) = 0, \quad (x_1, x_2, z) \in D, \quad (1)$$

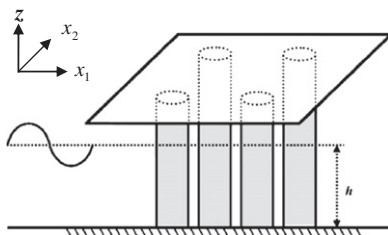


Fig. 1. Interaction of an incident water wave between four cylinders.

where ∇^2 is the Laplacian operator and D is the domain of interest. Based on the linearized water wave theory and using the technique of separation variables for space and time, we have

$$\Phi(x_1, x_2, z; t) = \text{Re}\{u(x_1, x_2)f(z)e^{-i\omega t}\}, \quad (2)$$

where

$$f(z) = \frac{-igA \cos hk(z+h)}{\omega \cos hkh}, \quad (3)$$

in which g is the gravity acceleration, A is the amplitude of incident wave, ω is the angular frequency, k represents the wave number and i is the imaginary number of $\sqrt{-1}$. The boundary condition of the total velocity potential on seabed is

$$\frac{\partial \Phi}{\partial z} \Big|_{z=-h} = 0, \quad (4)$$

and the linearized condition on the free surface is

$$\left(-\frac{\omega^2}{g} \Phi + \frac{\partial \Phi}{\partial z}\right) \Big|_{z=0} = 0. \quad (5)$$

In addition, the total velocity potential also satisfy the boundary condition on the wetted surface of all cylinders as follows:

$$\frac{\partial \Phi}{\partial n} = 0, \quad -h \leq z \leq 0, \quad (6)$$

where n stands for the normal vector of any cylinder with respect to its local polar coordinate system. The free-surface elevation in the time domain, $H(x_1, x_2, t)$, can be defined by

$$H(x_1, x_2, t) = \eta(x_1, x_2)e^{-i\omega t}, \quad (7)$$

where

$$\eta(x_1, x_2) = Au(x_1, x_2), \quad (8)$$

in which $\eta(x_1, x_2)$ is the free-surface elevation in the frequency domain, the total velocity potential $\Phi(x_1, x_2, z; t)$ can be expressed by

$$\Phi(x_1, x_2, z; t) = \Phi_R(x_1, x_2, z; t) + \Phi_I(x_1, x_2, z; t), \quad (9)$$

where the subscripts R and I denote the radiation field and the incident wave, respectively. Similarly, the function, $u(x_1, x_2)$, can also be expressed by

$$u(x_1, x_2) = u_R(x_1, x_2) + u_I(x_1, x_2). \quad (10)$$

The incident wave is given by

$$\Phi_I(x_1, x_2, z; t) = \frac{-igA \cos hk(z+h)}{\omega \cos hkh} e^{ik(x_1 \cos \theta_{inc} + x_2 \sin \theta_{inc})} e^{-i\omega t}, \quad (11)$$

where θ_{inc} is the incident angle. By substituting Eq. (2) into Eq. (1), the governing equation of the total velocity potential can be reduced to the two-dimensional Helmholtz equation as shown below:

$$(\nabla^2 + k^2)u(x_1, x_2) = 0, \quad (x_1, x_2) \in D, \quad (12)$$

where k is the wave number which satisfies the dispersion relationship

$$k \tan hkh = \frac{\omega^2}{g}. \quad (13)$$

The rigid cylinder yields the Neumann boundary condition as shown below:

$$\frac{\partial u(x_1, x_2)}{\partial n} = 0, \quad (x_1, x_2) \in B. \quad (14)$$

The dynamic pressure can be obtained by

$$p = -\rho_f \frac{\partial \Phi}{\partial t} = \rho_f g A \frac{\cos hk(z+h)}{\cos hkh} u(x_1, x_2) e^{-i\omega t}, \quad (15)$$

where ρ_f is the density of the fluid. The horizontal force can be obtained by integrating the dynamic pressure, p , over the wetted

surface of the cylinder. For the circular cylinder, the two components ($\cos \theta$, $\sin \theta$) of the first-order force \underline{x}^j on the j th cylinder are given as follows:

$$\underline{x}^j = -\frac{\rho_f g A a_j}{k} \tan hkh \int_0^{2\pi} u(x_1, x_2) \begin{Bmatrix} \cos \theta_j \\ \sin \theta_j \end{Bmatrix} d\theta_j, \quad j = 1, 2, 3, 4, \quad (16)$$

where a_j denotes the radius of the j th cylinder.

2.2. Dual boundary integral equations

The integral equations for the domain point can be derived from the third Green's identity, we have

$$2\pi u_R(x) = \int_B T(s, x) u_R(s) dB(s) - \int_B U(s, x) t_R(s) dB(s), \quad x \in D, \quad (17)$$

$$2\pi t_R(x) = \int_B M(s, x) u_R(s) dB(s) - \int_B L(s, x) t_R(s) dB(s), \quad x \in D, \quad (18)$$

where s and x are source and field points, respectively, $t_R(s) = (\partial u_R(s)) / \partial n_s$, \underline{n}_s denotes the unit outward normal vectors at source point s . The kernel function, $U(s, x) = -\frac{H_0^{(1)}(kr)}{2}$, is the fundamental solution which satisfies

$$(\nabla^2 + k^2)U(s, x) = 2\pi \delta(x - s), \quad (19)$$

where $\delta(x - s)$ denotes the Dirac-delta function, $H_n^{(1)}(kr) = J_n(kr) + iY_n(kr)$ is the n -th order Hankel function of the first kind, J_n is the n -th order Bessel function of the first kind, Y_n is the n -th order Bessel function of the second kind and $r = |x - s|$. The other kernel functions, $T(s, x)$, $L(s, x)$, and $M(s, x)$, are defined by

$$T(s, x) = \frac{\partial U(s, x)}{\partial n_s}, \quad (20)$$

$$L(s, x) = \frac{\partial U(s, x)}{\partial n_x}, \quad (21)$$

$$M(s, x) = \frac{\partial^2 U(s, x)}{\partial n_s \partial n_x}, \quad (22)$$

where \underline{n}_x denotes the unit outward normal vector at the field point x . By moving the field point to the boundary, Eqs. (17) and (18) reduce to

$$\pi u_R(x) = C.P.V. \int_B T(s, x) u_R(s) dB(s) - R.P.V. \int_B U(s, x) t_R(s) dB(s), \quad x \in B, \quad (23)$$

$$\pi t_R(x) = H.P.V. \int_B M(s, x) u_R(s) dB(s) - C.P.V. \int_B L(s, x) t_R(s) dB(s), \quad x \in B, \quad (24)$$

where R.P.V., C.P.V. and H.P.V. denote the Riemann principal value (Riemann sum), the Cauchy principal value and the Hadamard principal value (or the Hadamard finite part), respectively. Once the field point x is located outside the domain ($x \in D^c$), we obtain the dual null-field integral equations as shown below:

$$0 = \int_B T(s, x) u_R(s) dB(s) - \int_B U(s, x) t_R(s) dB(s), \quad x \in D^c, \quad (25)$$

$$0 = \int_B M(s, x) u_R(s) dB(s) - \int_B L(s, x) t_R(s) dB(s), \quad x \in D^c, \quad (26)$$

where D^c is the complementary domain. Eqs. (17), (18), (25) and (26) are conventional formulations that the collocation point cannot be located on the real boundary. Singularity occurs and concept of principal values is required once Eqs. (23) and (24) are considered. The flux $t_R(s)$ is the directional derivative of $u_R(s)$ along the outer normal direction at s . For the interior point, $t_R(x)$ is artificially defined. For example, $t_R(x) = \partial u_R(s) / \partial x_1$, if $n = (1, 0)$ and $t_R(x) = \partial u_R(x) / \partial x_2$, if $n = (0, 1)$ where (x_1, x_2) is the coordinate of the

field point x . The dual boundary integral equations can be discretized by using N constant elements for one cylinder, and then algebraic systems can be obtained as shown below:

$$[T]\{u_R\} = [U]\{t_R\}, \quad (27)$$

$$[M]\{u_R\} = [L]\{t_R\}, \quad (28)$$

where $[U]$, $[T]$, $[L]$ and $[M]$ are the influence matrices.

3. Suppression of the fictitious frequencies

3.1. Burton and Miller method

In the Burton and Miller method, we combined the singular integral equation and its normal derivative (hypersingular integral equation) with an imaginary constant. This method can construct a non-singular matrix for any wave number, hence a unique solution can be obtained. The formulation of the Burton and Miller method is shown below:

$$\left[[T] + \frac{i}{k} [M] \right] \{u_R\} = \left[[U] + \frac{i}{k} [L] \right] \{t_R\}. \quad (29)$$

3.2. CHIEF method

In either the singular or the hypersingular formulation, the influence matrix becomes singular or ill-posed, when the wave number is close to the fictitious frequency. This means that the rank of the influence matrices is deficient. By using the CHIEF idea to put the collocation point on the null-field (Eq. (25)), the additional constraint equation can be obtained as follows:

$$\langle T^c \rangle \{u_R\} = \langle U^c \rangle \{t_R\}, \quad (30)$$

where $\langle U^c \rangle \psi$ and $\langle T^c \rangle \psi$ are the influence row vectors. By combining Eq. (30) with the discrete system of Eq. (27), we have an over-determined system:

$$\begin{bmatrix} T \\ \langle T^c \rangle \end{bmatrix} \{u_R\} = \begin{bmatrix} U \\ \langle U^c \rangle \end{bmatrix} \{t_R\}. \quad (31)$$

Eq. (31) can yield a unique solution if the proper CHIEF points are selected. For a circular cylinder case, one can adopt one interior CHIEF point $x_1(r_1, \phi_1)$, where r_1 is shown in Fig. 2(a). Based on the singular value decomposition (SVD) technique [33], a CHIEF point can obtain a discriminant, Δ :

$$\Delta = \langle T^c \rangle \{u_R\} = \pi^2 r_1 H_n'(1)(ka) J_n(kr_1) e^{in\phi_1}, \quad (32)$$

For the fictitious wave number of multiplicity one $k_{0,m}^f$, the superscript f denotes the wave number where the "fictitious" mode appears and $k_{0,m}$ denotes the m th zero of the zeroth order Bessel function (J_0). If the selected interior point, $x_1(r_1, \phi_1)$, satisfies

$$k_{0,m}^f r_1 = k_{0,p}, \quad (m > p), \quad (33)$$

where $k_{0,p}$ denotes the p th zeros for the J_0 function, then the fictitious wave number, $k_{0,m}^f$ cannot be alleviated. For the fictitious roots of multiplicity two ($n > 0$), the selected interior point,

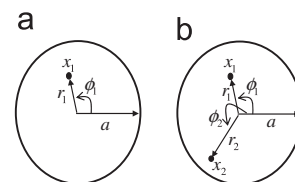


Fig. 2. Sketch of CHIEF point. (a) One CHIEF point ($x_1 = (r_1, \phi_1)$) (b) Two CHIEF points ($x_1 = (r_1, \phi_1)$, $x_2 = (r_2, \phi_2)$)

$x_1(r_1, \phi_1)$, satisfying

$$k_{n,m}^f r_1 = k_{n,p}, \quad (m > p), \quad (34)$$

is invalid to suppress the fictitious wave number, $k_{n,m}^f$. In case of a fictitious frequency with multiplicity two ($J_n(k)=0, n \geq 1$), the rank is reduced by two. One point provides at the most one valid constraint equation. One point cannot filter out the fictitious wave number of multiplicity two, so an additional independent equation is required by adding one more CHIEF point. If one adopts another interior point $x_2(r_2, \phi_2)$ as shown in Fig. 2(b), we have the discriminant, Δ :

$$\Delta = \langle T^c \rangle \{u_R\} = i2r_1 r_2 H'_n(1)(ka) H'_n(1)(ka) J_n(kr_1) J_n(kr_2) \sin(n\phi), \quad (35)$$

where $\phi = \phi_1 - \phi_2$ indicates the intersecting angle between the two interior points. The discriminant Δ indicates an index to check the validity of CHIEF point by the following criterion:

- (1) If the two points with the intersection angle ϕ produce $\phi = \pi$, such that $\sin(n\phi) = \sin(\pi) = 0$, i.e., $\phi = \pi/n$, it fails to alleviate the irregular frequency in the root of double multiplicity for $J_n, n \geq 1$.
- (2) If the position of two points satisfy $J_n(kr_1) = 0$ or $J_n(kr_2) = 0, n = 1, 2, 3, \dots$, then it also fails to alleviate the irregular frequency in the root of multiplicity two for J_n .
- (3) No more than two points are needed if points are properly chosen.

4. Illustrative examples

4.1. Case 1: Fictitious frequency for water wave impinging on a circular cylinder using the DBEM

In this case, we consider the water wave problem by a vertical rigid circular cylinder with radius a ($a=1.0$) as shown in Fig. 3. MacCamy and Fuchs [1] derived the exact solution of the horizontal force on the bottom mounted on seabed cylinder as shown below:

$$F_x = \frac{4\rho_f g A \tan hkh}{k^2 H_1^{(1)}(ka)}. \quad (36)$$

Au and Brebbia [36] also solved this problem by using constant, linear and quadratic boundary elements. However, the irregular value was not addressed in their work. The nondimensional resultant force ($F_N = F_x / \{\rho_f g A h \tan h(kh)/kh\}$) versus ka is plotted as shown in Fig. 4. The positions where the irregular values occur are found in Fig. 4 by using either the UT or the LM formulation alone. It is found that no irregular wave number occurs, if the Burton and Miller method is adopted as shown in Fig. 4. It is found that irregular values happened to be zeros of the n -th order Bessel function of the first kind for the UT formulation ($J_n(ka) = 0$), while the LM formulation has the irregular values for zeros of the derivatives of Bessel function ($J'_n(ka) = 0$) as shown in Fig. 4. In Fig. 4, the data in the parentheses are analytical solutions

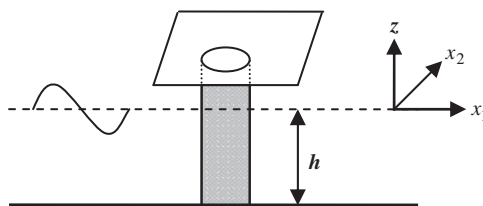


Fig. 3. Problem sketch of water wave with a vertical cylinder.

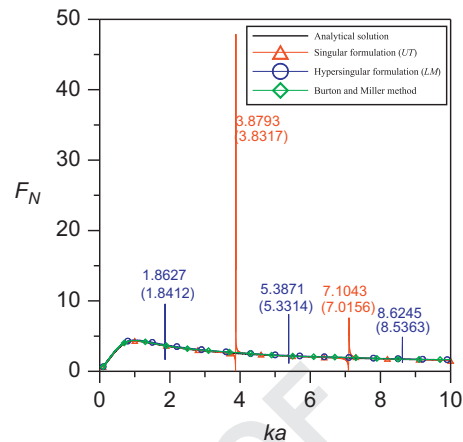


Fig. 4. F_N versus ka using the UT, LM formulations and the Burton and Miller method.

Table 2
Zeros of the Bessel function $J_{n,m}(k)$.

n	m			
	0	1	2	3
1	2.40	3.83	5.13	6.38
2	5.52	7.01	8.41	9.76

Table 3
Zeros of the Bessel function $J'_{n,m}(k)$.

n	m			
	0	1	2	3
1	0	1.84	3.05	4.20
2	3.83	5.33	6.70	8.01

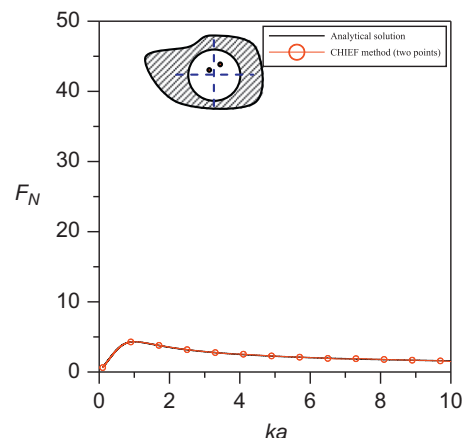


Fig. 5. F_N versus ka using two CHIEF points to suppress of the fictitious frequency.

for ka corresponding to zeros of $J_n(ka)$ and $J'_n(ka)$. Zeros of the Bessel function $J_n(ka)$ and $J'_n(ka)$ are shown in Tables 2 and 3, respectively. In Fig. 4, it shows the “resultant force” instead of the direct output of boundary potential or boundary potential gradient. Since the resultant force is determined by Eq. (16) for the

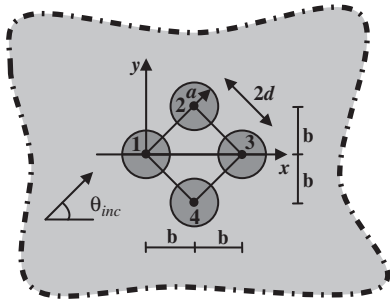
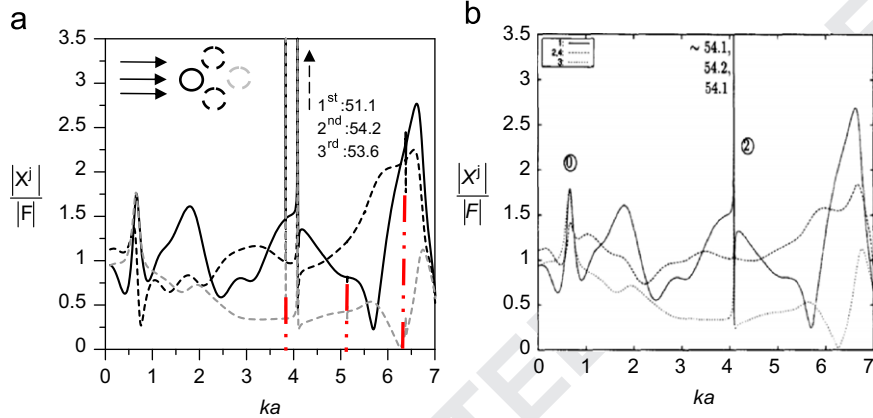


Fig. 6. Interaction of an incident water wave among four cylinders.

projection on cosine and sine functions. Based on the orthogonality condition of Fourier bases, it is obvious that only the fictitious frequency $J_1(ka) = 0$ and $J_1'(ka) = 0$ may appear. It is a root of multiplicity two. The eigen mode of the root of multiplicity two can be expressed by sine and cosine functions. For the eigen mode of the root of multiplicity two, it has at least one angular nodal line and the nodal line can be rotated. The CHIEF method is also adopted to deal with the problem of nonunique solution. When we add only one CHIEF point at (0.2, 0.3) to suppress the fictitious frequencies, it fails since it is a root of multiplicity two for $J_n(ka) = 0, n \geq 1$. One point provides at most one constraint equation and cannot filter out the root of multiplicity two, we



Q6 Fig. 7. Resultant force of the cylinders versus ka by using the (a) UT formulation and (b) Evans and Porter [12]. (For interpretation of the references to color in this figure, the reader is referred to the web version of this article.)

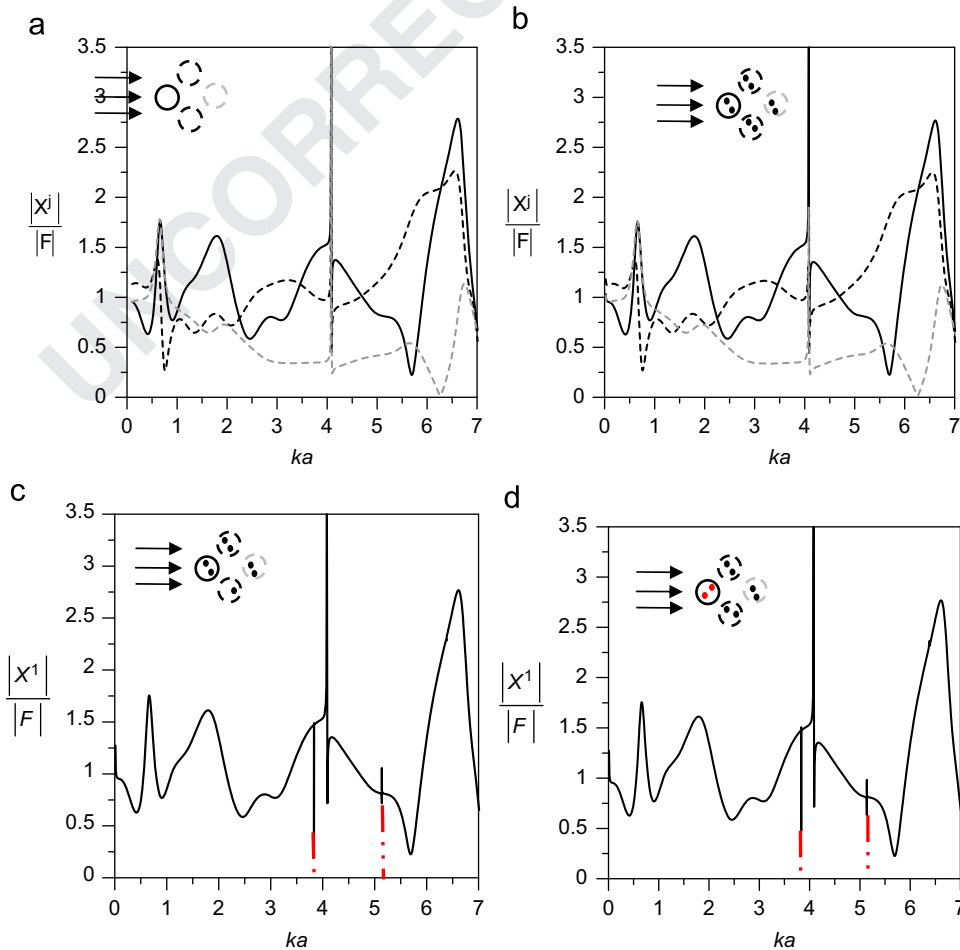


Fig. 8. Suppression of the fictitious frequency by using (a) Burton and Miller (b) CHIEF methods (c) CHIEF method (7 CHIEF points) and (d) Failure CHIEF points (8 points containing failure positions).

must add at least two CHIEF points to suppress the fictitious frequencies. The result of using two CHIEF points is shown in Fig. 5 and no fictitious frequencies are observed.

4.2. Case 2: Water wave problem by an array of four circular cylinders using the DBEM

We consider the water wave problem by an array of four bottom-mounted vertical rigid circular cylinders with the same radius a ($a=1.0$) located at the vertices of a square $(0, 0)$, (b, b) , $(2b, 0)$, $(b, -b)$ and $a/d=0.8$ as shown in Fig. 6. By considering the incident wave in the direction of zero degrees, Fig. 7(a) shows the force ratio of the cylinders in the direction of incident wave versus the wave number by using the singular (UT) formulation. It is interesting to find that two kinds of peak occur. It becomes very important to distinguish the source of near-trapped mode or numerical instability. One kind of peak appears at the corresponding wave number which happens to be zeros of the Bessel function $J_n(ka)$, corresponding to the fictitious k_f (3.83, 5.13 and 6.38), as shown by red line in Fig. 7(a). The other peak occurs at the wave number of $k=4.083$ which is physically realizable as a near-trapped mode. It can be found that the peak force on the first cylinder is about 51 times of an isolated cylinder and the second cylinder and the third cylinder are 54.2 and 53.6 times of an isolated cylinder, respectively. This near-trapped mode ($ka=4.084$) was also recorded by Evans and Porter [12],

Table 4 Improvement of rank deficiency by using valid CHIEF points.

Number of valid CHIEF points	Locations	Rank of the influence matrix (N is the total number of elements)
0	-	$N-8$
1	(0.30, 0.30)	$N-7$
2	(0.35, 0.70)	$N-6$
3	(2.07, 2.07)	$N-5$
4	(2.11, 2.46)	$N-4$
5	(3.83, 0.30)	$N-3$
6	(3.88, 0.70)	$N-2$
7	(2.06, -1.46)	$N-1$
8	(2.11, -1.06)	N

as shown in Fig. 7(b). It is explained that fictitious frequencies occur when we employ BEM to solve exterior Helmholtz problems. It belongs to numerical resonance instead of physical phenomenon.

4.2.1. Suppression of the fictitious frequency

We employ the Burton and Miller method and the CHIEF method to suppress the fictitious frequencies. Fig. 8(a) shows the ratio of force on the cylinders versus ka by using the Burton and Miller method. Since the zeros of the Bessel functions and their derivatives cannot simultaneously be the same k value, the stable solution can be obtained by using the Burton and Miller method.

The highly rank-deficient matrices for four identical radius of cylinders are numerically examined and the rank is improved by adding valid CHIEF points as shown in Table 4. In Table 4, the range of ka is from 0.01 to 7.0, only 5 fictitious frequencies in the range are found in Table 2. If the eigen mode only has radial nodal lines, that is the fictitious frequency is a root of $J_0(k)=0$, only 4 trial CHIEF points are sufficient to suppress the appearance of fictitious wave number. Otherwise, at least 8 CHIEF points are required. Fig. 8(b) shows the resultant force versus ka by using the CHIEF method. If the CHIEF points are properly chosen, only at least eight CHIEF points for four identical cylinders are needed. Therefore, all fictitious frequencies are suppressed. If the invalid CHIEF points or insufficient CHIEF points are chosen, Fig. 8(c) and (d) show the resultant force versus ka . The fictitious frequency at $k=3.83$ and $k=5.13$ also exist and cannot be suppressed due to the failure CHIEF points $x_1(0.3,0.3)$ and $x_2(-0.3,-0.3)$, where the intersection angle for these points is equal to π and locate on the nodal line as shown in Fig. 9(a) and (b), respectively. Furthermore, results of the Burton and Miller method and CHIEF method agree well with those by Evans and Porter [12].

4.2.2. Parameter study on the near-trapped mode

Here, we study the occurrence of near-trapped mode and fictitious frequency by changing two parameters. First, we consider the effect of radius. For numerical experiments by changing the radius of first cylinder a to $1.2a$, the fictitious frequency occur at zeros of Bessel function ($J_n(ka)=0$ and $J_n(1.2ka)=0$, $n=0,1,2\dots$) for the singular (UT) formulation, respectively. In Fig. 10(a), it shows that fictitious frequencies still appear due to the radius of $r=a$, corresponding to the fictitious wave number k_f (5.13 and

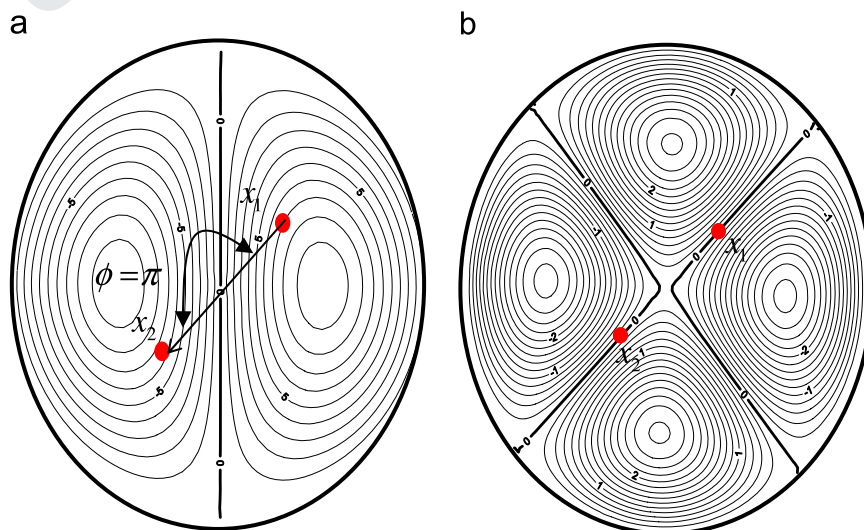


Fig. 9. Eigen modes for the Dirichlet problem of a circle (a) $k=3.83$ and (b) $k=5.13$.

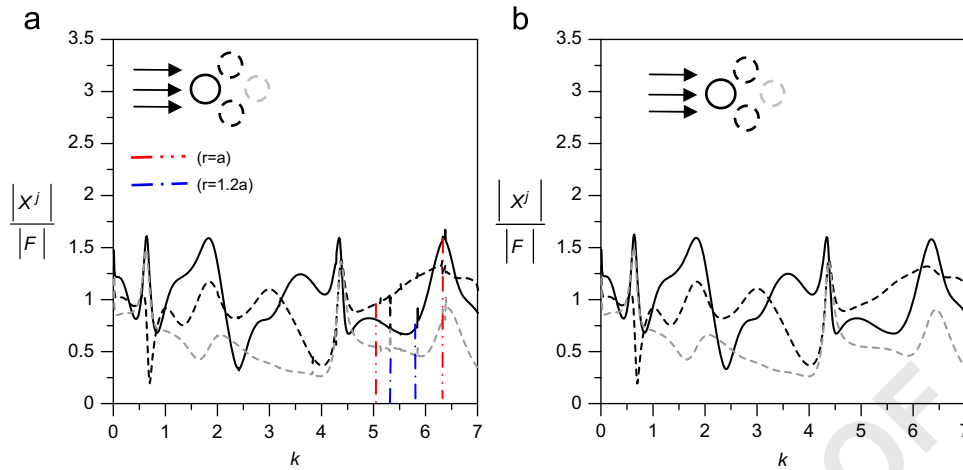


Fig. 10. Resultant force of the cylinder versus the k , by changing the radius a to $1.2a$ by using (a) *UT* formulation and (480 elements) (b) Burton and Miller method (480 elements). (For interpretation of the references to color in this figure, the reader is referred to the web version of this article.)

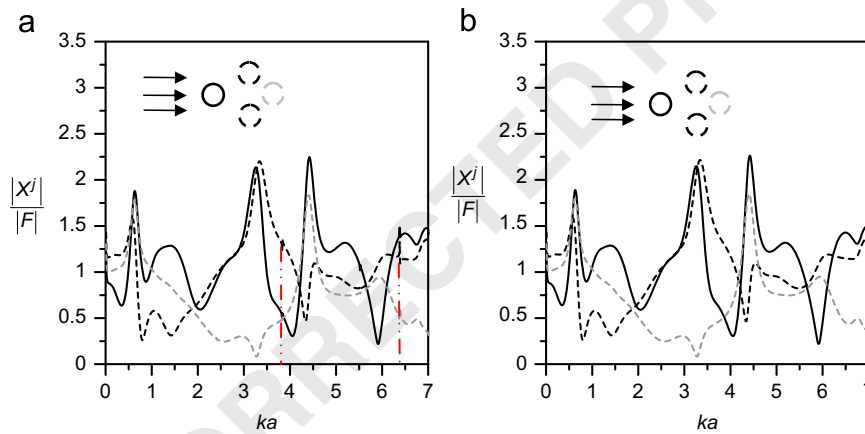


Fig. 11. Resultant force of the cylinders versus the ka , by changing the position ($0.5a$) of the first cylinder by using (a) *UT* formulation and (480 elements) (b) Burton and Miller method (480 elements).

Table 5

Force ratio of the first cylinder by changing the radius of the first cylinder to destroy the periodical setup ($ka=4.083$).

Changing radius	$a_1=0.6a$	$a_1=0.7a$	$a_1=0.8a$	$a_1=0.9a$	$a_1=a$	$a_1=1.1a$	$a_1=1.2a$	$a_1=1.3a$	$a_1=1.4a$
Normalized force ratio	1.97	1.82	1.577	1.32	51.1*	1.12	1.049	1.038	1.069

where * means near-trapped mode and a_1 is the radius of the first cylinder.

Table 6

Force ratio of the first cylinder by moving center of the first cylinder to destroy the periodical setup ($ka=4.083$).

New center	$(-0.4a,0)$	$(-0.3a,0)$	$(-0.2a,0)$	$(-0.1a,0)$	$(0,0)$	$(0.1a,0)$	$(0.2a,0)$	$(0.3a,0)$	$(0.4a,0)$
Normalized force ratio	0.54	0.95	1.15	1.20	51.1*	1.21	1.11	1.01	0.93

where * means trapped mode.

6.38), as shown by the red line, and $r=1.2a$, corresponding to the fictitious wave number $k_j/1.2a$ ($6.38/1.2=5.31$, $7.016/1.2=5.84$) as shown by the blue line in Fig. 10(a). Fig. 10(b) shows the force on the first cylinder versus k by using the Burton and Miller method. It can be found that the ratio of force for the near-trapped mode becomes smaller.

Secondly, we consider the effect of spacing between cylinders. To study the effect of spacing on the near-trapped mode, we change the position of the first cylinder. It is found that the location of fictitious frequency remains at the same position by using the *UT* formulation. However the ratio of the force for the near-trapped mode becomes smaller as shown in Fig. 11(a).

Fig. 11(b) shows the ratio of force on the cylinder versus the ka by using the Burton and Miller method. The amplitude of the near-trapped mode also becomes smaller. Tables 5 and 6 indicate that the peak value for the near-trapped mode is reduced significantly due to the perturbation of either radius or position of the center of the first cylinder.

4.3. Case 3: Water wave problem by an array of four square cylinders using the DBEM

To see the generality of the DBEM, we consider the water wave problem by an array of four bottom-mounted vertical rigid square cylinders with the same length d ($d=1.0$) located at the vertices of a square as shown in Fig. 12. The angle of the incident wave is 45 degrees. Fig. 13(a) and (b) show the force on the first cylinder versus the wave number by using the UT formulation and the Burton and Miller method, respectively, where $R = |X_1|/|F_0|$ and F_0 is the horizontal force of an isolated square cylinder. In Fig. 13(a),

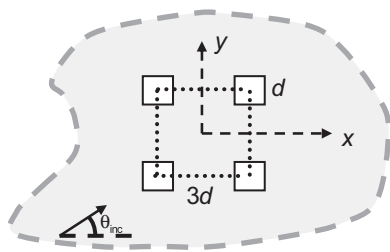


Fig. 12. Interaction of an incident water wave with four square cylinders.

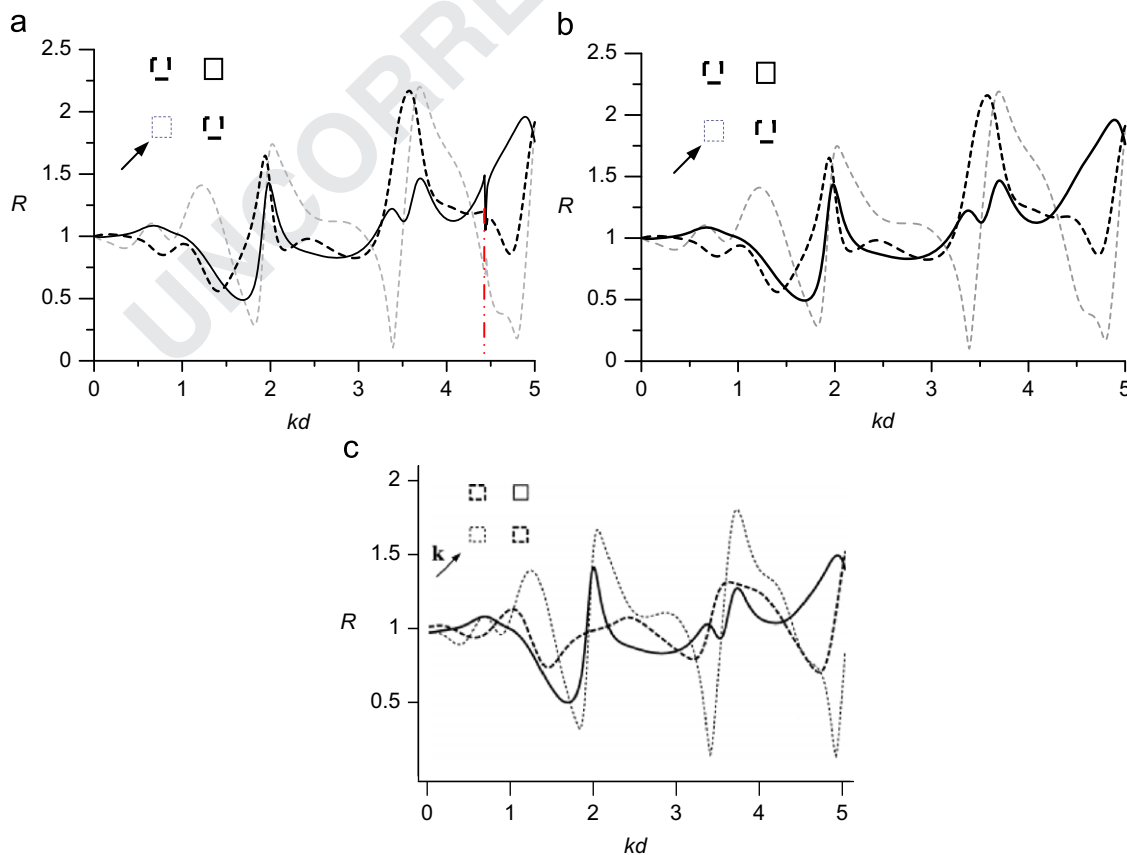


Fig. 13. Resultant force of the four square cylinders versus kd by using (a) UT formulation (160 elements) (b) Burton and Miller method (160 elements) and (c) Stojek et al. [36].

it is found that the fictitious frequency appears at the corresponding wave number $kd=4.44$ which happens to be the eigen value of square domain (analytical solution is $k_{mn} = \sqrt{(m/d)^2 + (n/d)^2}$, $m, n=0,1,2, \dots$). Although there is some deviations for the larger k value, agreeable results between our approach and Trefftz-type FEM method [37] are found, as shown in Fig. 13(c).

5. Conclusions

In this paper, we applied the DBEM to solve water-wave scattering problems containing one-circular cylinder, four-circular cylinders and four-square cylinders. Discussions on the physical phenomena of near-trapped mode as well as the numerical phenomena due to fictitious frequency in the DBEM were both addressed. Near-trapped modes and the fictitious frequencies are physically and mathematically realizable, respectively. For the circular cylinder case, the fictitious frequencies happen to be zeros of Bessel functions and their derivatives for the singular (UT) and the hypersingular (LM) equations, respectively. Two approaches, the CHIEF method and the Burton and Miller approach, were successfully to suppress the appearance of fictitious frequencies. Highly rank-deficiency matrices were observed for four identical circular cylinders and more CHIEF points were required. Besides, the effects of radius on the fictitious frequency as well as the effect of spacing on the near-trapped mode were studied. Finally, resultant forces on each cylinder were given to illustrate the effect of disorder of the periodical layout on the near-trapped modes.

References

- [1] MacCamy RC, Fuchs RA. Wave force on piles: a diffraction theory. Washington, D.C: US Army, Coastal Engineering Research Center, Technical Memorandum; 1954.
- [2] Spring BH, Monkmeyer PL. Interaction of plane waves with vertical cylinders. Proc 14th Int Conf Coastal Eng 1974;1828–1845.
- [3] Twersky V. Multiple scattering of radiation by an arbitrary configuration of parallel cylinders. J Acoust Soc Am 1952;24(1):42–46.
- [4] Duclos G, Clément AH. Wave propagation through arrays of unevenly spaced vertical piles. Ocean Eng 2004;31:1655–1668.
- [5] Simon MJ. Multiple scattering in arrays of axisymmetric wave-energy devices. J Fluid Mech 1982;120:1–25.
- [6] McIver P, Evans DV. Approximation of wave forces on cylinder arrays. Appl Ocean Res 1984;6(2):101–107.
- [7] Linton CM, Evans DV. The interaction of waves with arrays of vertical circular cylinders. J Fluid Mech 1990;215:549–569.
- [8] Linton CM, Evans DV. Corrigendum: the interaction of waves with arrays of vertical circular cylinders. J Fluid Mech 1990;218:663.
- [9] Chen JT, Lee YT, Lin YJ. Interaction of water waves with arbitrary vertical cylinders using null-field integral equations. Appl Ocean Res 2009;31:101–110.
- [10] Chen JT, Lee JW. Water wave problems using null-field boundary integral equations: ill-posedness and remedies. Appl Anal. in press.
- [11] Liu L, Hussein MI. Wave motion in periodic flexural beams and characterization of the transition between Bragg scattering and local resonance. J Appl Mech 2012;79:1–17.
- [12] Evans DV, Porter R. Near-trapping of waves by circular arrays of vertical cylinders. Appl Ocean Res 1997;19:83–99.
- [13] Sphaier S, Yeung R. Wave-interference effects on a truncated cylinder in a channel. J Eng Math 1989;23:95–117.
- [14] Kashiwagi M. 3-D Calculation for multiple floating bodies in proximity using wave interaction theory. Int J Offshore Polar Eng 2008;18(1):14–20.
- [15] Kashiwagi M. Wave-induced local steady force on a column-supported very large floating structure. Int J Offshore Polar Eng 2002;12(2):98–104.
- [16] Kagemoto H, Murai M, Saito M, Molin B, Malenica S. Experimental and theoretical analysis of the wave decay long a long array of vertical cylinders. J Fluid Mech 2002;456:113–135.
- [17] Ohl COG, Eatock Taylor R, Taylor PH, Borthwick AGL. Water wave diffraction by a cylinder array. Part 1. Regular waves. J Fluid Mech 2001;442:1–32.
- [18] Meylan MH, Eatock Taylor R. Time-dependent water-wave scattering by arrays of cylinders and the approximation of near trapping. J Fluid Mech 2009;631:103–125.
- [19] Maniar HD, Newman JN. Wave diffraction by a long array of cylinders. J Fluid Mech 1997;339:309–330.
- [20] Thompson I, Linton CM, Porter R. A new approximation method for scattering by long finite arrays. Q J Mech Appl Math 2008;25:333–352.
- [21] Evans DV, Porter R. Trapped modes about multiple cylinders in a channel. J Fluid Mech 1997;339:331–356.
- [22] Yao Y, Tulin M, Kolani A. Theoretical and experimental studies of three-dimensional wavemaking in narrow tanks, including nonlinear phenomena near resonance. J Fluid Mech 1994;276:211–232.
- [23] Linton CM, McIver P. Embedded trapped modes in water waves and acoustics. Wave Motion 2007;45:16–29.
- [24] Chen JT, Chen CT, Chen KH, Chen IL. On fictitious frequencies using dual bem for non-uniform radiation problems of a cylinder. Mech Res Commun 2000;27(6):685–690.
- [25] Chen JT, Liang MT, Chen IL, Chyuan SW, Chen KH. Dual boundary element analysis of wave scattering from singularity. Wave Motion 1999;30(4):367–381.
- [26] Chen JT, Lin JH, Kuo SR, Chyuan SW. Boundary element analysis for the Helmholtz eigenproblems with multiply-connected domain. Proc R Soc London Ser A 2001;457(2014):2521–2546.
- [27] Chen JT, Lin SY, Chen IL, Lee YT. Mathematical analysis and numerical study for free vibration of annular plates using BIEM and BEM. Int J Numer Methods Eng 2006;65:236–263.
- [28] Dokumaci E. A study of the failure of numerical solutions in boundary element analysis of acoustic radiation problems. J Sound Vib 1990;139(1):83–97.
- [29] Juhl P. A numerical study of the coefficient matrix of the boundary element method near characteristic. J Sound Vib 1994;175(1):39–50.
- [30] Chen JT, Chen KH, Chen IL, Liu LW. A new concept of modal participation factor for numerical instability in the dual BEM for exterior acoustics. Mech Res Commun 2003;26(2):161–174.
- [31] Burton AJ, Miller GF. The application of integral equation methods to numerical solution of some exterior boundary value problems. Proc R Soc London Ser A 1971;323:201–210.
- [32] Schenck HA. Improved integral formulation for acoustic radiation problem. J Acoust Soc Am 1968;44:41–58.
- [33] Chen IL, Chen JT, Liang MT. Analytical study and numerical experiments for radiation and scattering problems using the CHIEF method. J Sound Vib 2001;248(5):809–828.
- [34] Schenck HA. Helmholtz integral formulation of the sonar equations. J Acoust Soc Am 1986;79(5):1423–1433.
- [35] Dokumaci E, Sarigul AS. Analysis of the near field acoustic radiation characteristics of two radially vibrating spheres by the Helmholtz integral equation formulation and a critical study of the efficacy of the "CHIEF" over determination method in two-body problems. J Sound Vib 1995;187(5):781–798.
- [36] Au MC, Brebbia CA. Diffraction of water waves for vertical cylinders using boundary elements. Appl Math Model 1983;1(7):106–114.
- [37] Stojek M, Markiewicz M, Mahrenholtz O. Diffraction loads on multiple vertical cylinders with rectangular cross section by Trefftz-type finite elements. Comput Struct 2000;75:335–345.